Laser-radiation tolerance of promising materials of IR optics. Part 1. Material damage mechanisms

S.G. Kazantsev

RADUGA State Scientific Research Laser Center, Raduzhnyi, Vladimir Region

Received January 22, 2003

Laser induced damage of ZnSe, CdTe, Ge, KRS-5, KCl, NaCl, and BaF_2 single crystals was investigated with the pulsed CO, CO_2, HF, DF, Nd^{3+}YAG lasers, as well as repetitively pulsed CO and CO_2 lasers. Physical and mathematical models of destruction of transparent dielectrics and semiconductors were developed. The laser-radiation tolerance of IR materials was found to correlate with the fundamental characteristics: refractive index, bandgap, spectral range, crystal lattice energy, anionic and cationic radii, and the element number in the Periodic Table.

The development of laser technologies of material processing in vacuum and gas media (surface modification and hardening, melting, evaporation, welding, cutting, marking, etc.), as well as works on inertial nuclear fusion and some other practical applications of quantum electronics have lead to advent of mid-IR gas lasers with the output radiation intensity up to ~10^6–10^{10} W · cm^{-2} in the pulsed mode and the mean output power up to hundreds of kilowatts in the repetitively pulsed mode, the pulse duration ~10^{-9}–10^{-3} s and the aperture of 3 to 30 cm (Refs. 1–4). The need in shaping such high-power radiation in space and delivering it to objects under study required developing reliable and long-lived wide-aperture transmitting optics: laser windows, prisms, wedges, and other elements of optical instruments. This, in its turn, caused the need in experimental investigations on laser-radiation tolerance of promising IR materials (ZnSe, CdTe, KCI, NaCl, KRS-5, BaF_2, etc.) at real aperture values.[1,6–9]

Surface damage of optical elements

Surface damages of optical elements that arise under the exposure to wide-aperture pulsed radiation with λ = 1.06–10.6 μm and duration of 0.1 μs–10 ms are crack network with the crack depth of 0.1–1 mm and length of 1–100 mm. In semiconductor crystals, craters and caverns with the size up to 1–3 mm arise as well. Crack orientation is determined by the crystal structure and symmetry. The distribution of defects on the surface and the degree of its damage correlate with the intensity and size of plasma formations arising at optical breakdown. The threshold for appearance of surface damage depends on the parameters of laser radiation and the material of an optical element.

Under the exposure to radiation with the wavelength λ = 10.6 μm and the pulse duration $\tau \sim 1$ μs, KRS-5 single crystals are damaged at the energy density W_{ts} ~ 1–4, KCl – 1–7, NaCl – 1–9, BaF_2 – 6–12, Ge and CdTe – 0.5–4, ZnSe – 0.5–6 J · cm^{-2} (intensity $q_{ts} \sim W_{ts}/\tau$) [Refs. 1, 2, 6–9].

Using the methods of high-speed photorecording and spectroscopy of temporal, spatial, and spectral characteristics of plasma formations arising at optical breakdown near the surface of optical elements, we revealed the main regularities in the appearance and development of optical breakdown near the surface and proposed the surface damage mechanism.[1,2,10,12]

A plasma formation arises at the distance h ~ 3–5 mm from the optical element surface with a delay Δt_f relative to the leading front of the laser pulse. The maximum height of the plasma torch achieves 20–50 mm, and its temperature is (5–20)·10^3 K. The value of Δt_f depends on the maximum intensity of laser radiation q_{max} and the duration of the leading front of the laser pulse $\Delta\tau$. For $\Delta\tau$ ~ 200 ns the dependence $\Delta t_f \sim q_{max}^{-0.3}$ exists. The initial speed of the front of the near-surface plasma torch in first 0.5 μs after the onset of optical breakdown achieves the values of 5–8 km · s^{-1}, then the speed gradually decreases down to 3–4 km · s^{-1} for next 1–1.5 μs and down to 1–2 km · s^{-1} for 10 μs more. After 1 to 3 μs after the initial plasma formation, the surface of an optical element experiences, in addition to laser and UV exposure, the effect of high-temperature front of the shock wave propagating at a supersonic speed. The delay of the acoustic response Δt_p to this effect relative to the leading front of the laser pulse is ~ 2–4 μs, and it is a superposition of the following intervals: delay of the initial plasma formation (Δt_f ~ 0.2–1 μs), time needed for the front of the shock wave to pass the distance between the breakdown site and the surface of the optical element

0235-6880/03/04 359-07 $02.00

(1–3 μs), the time for acoustic wave propagation in the crystal from the area of shock wave effect to a piezosensor (~ 1–2 μs) (Refs. 1 and 2).

In integral emission spectra of plasma formations, the most intense lines are the broadened lines of double ionized air components, mostly NII and OII, emission lines of atoms of the material, the optical element consists of, as well as the H_α line characteristic of water adsorbed on the surface of optical elements. The emission spectrum of air components is observed already in the first microsecond of optical breakdown, while the H_α line appears with the delay ~ 2–3 μs after the initial plasma formation and becomes most intense. Propagation of the shock wave is accompanied by fast cooling of the rarefied gas in the near-surface area, and the high intensity of radiation from the plasma formation keeps only against the background of plasma torch, and the H_α line is seen rather clearly.[1,2]

Thus, optical breakdown appears in the air–gas mixture without participation of adsorbents. The following sharp increase of the intensity of the H_α line is indicative of the active interaction of the adsorbent vapor with the laser radiation and the UV radiation from the plasma formation, which is accompanied by photoionization, heating, and removal of adsorbent vapor by the front of the shock wave of the expanding plasma torch.

The separation into stages in the proposed physical model of the multistage surface damage mechanism is determined by the characteristics of factors affecting the surface of an optical element (Table).

The experimental data obtained allowed us to formulate some observations important for practice, as well as to explain the following regularities[10,12]:

1. Based on the model of interference of the incoming laser radiation and that reflected from sides of the optical element, the correlation was found between the surface damage thresholds q_{ts} and the index of refraction and reflection coefficient:

$$q_{ts} \sim (n+1)^2/4n^2 \quad (1)$$

or

$$q_{ts} \sim (1 + R^{1/2})^{-2}, \quad (2)$$

where n and R are, respectively, the index of refraction and reflection coefficient. The obtained correlation agree with the experimental values of the surface damage thresholds of ionic and semiconductor crystals and metal mirrors in the region of relatively high reflectivity $R > 0.1$ and high values of the refractive index $n > 1.5$.

2. The inverse λ squared dependence of the surface damage thresholds for the material of one type is explained by the fact that the breakdown occurs in the air–gas medium, and the strength of the threshold field of optical breakdown ε at avalanche ionization is proportional to its frequency ν. Taking into account that $\varepsilon \sim q^{1/2}$ and $\nu \sim \lambda^{-1}$, we obtain

$$q_{ts} \sim \lambda^{-2}. \quad (3)$$

Table. Mechanism of damage of optical element surface by pulsed laser radiation of microsecond duration

Stage	Main physical phenomena characteristic of this stage	Active factor	Stage duration, μs
Appearance of optical breakdown	Interference of incident and reflected laser radiation, optical breakdown in air–gas medium at a distance from the surface	Laser radiation	0.2–1 ($\Delta t_f \sim q_{max}^{-n}$)
Development of plasma torch	Heating of breakdown plasma by laser radiation up to 5–20 000 K, expansion of the shock wave front with the speed of 3–10 km · s^{-1}	Laser radiation + UV radiation of plasma	1–3
Contact of the surface with the front of shock wave of breakdown plasma	Thermal and acoustic shock, sublimation of adsorbent vapor from the surface	Laser radiation + UV radiation of plasma + thermal and acoustic shock	3–8
Surface damage	Interaction of ionized adsorbent vapor with laser radiation and breakdown plasma, heating, and re-emission in the visible and UV regions. Local heating of the near-surface zone of the optical element, appearance of the sharp temperature gradient, surface cracking	Laser radiation + UV radiation of plasma	> 10

3. For materials with $R < 0.1$ and $n < 1.5$, the farther in the UV region is the bandgap absorption boundary λ_{uv} (the larger is the bandgap E_g), the higher is the surface damage threshold (Fig. 1).

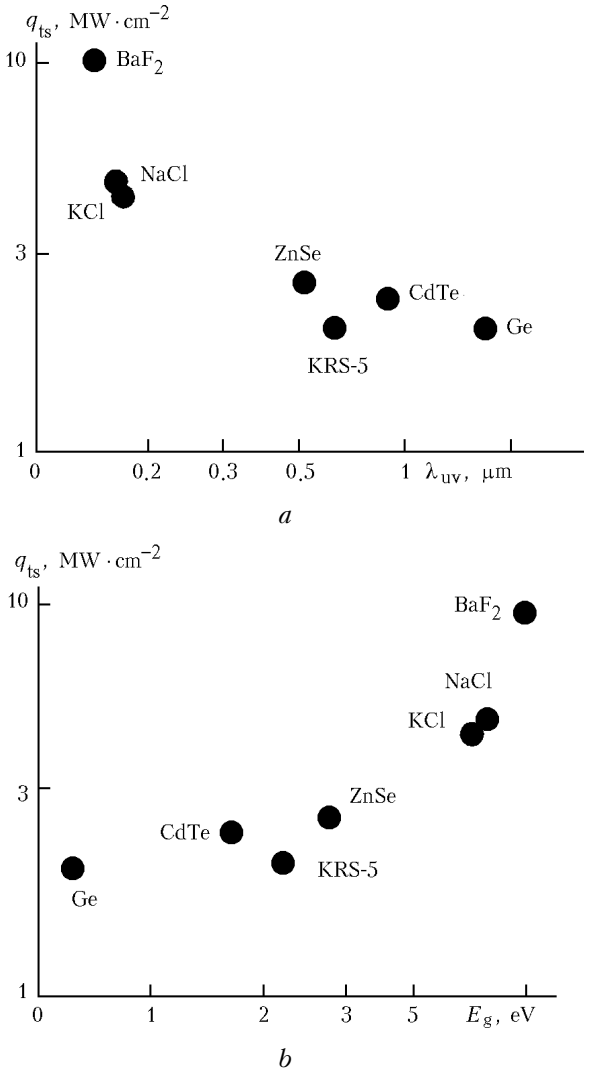

Fig. 1. Experimental values of surface damage thresholds for single crystals and their dependence on the bandgap absorption boundary (*a*) and the bandgap (*b*).

Since the maximum of emission spectrum of a plasma formation having the temperature ~ (5–20) · 10^3 K is in the range from 0.6 and down to 0.15 μm, the near-surface layer of most semiconductor crystals (λ_{uv} ~ 0.5–1.8 μm) absorbs the larger fraction of the energy emitted by the plasma formation than in ionic crystals (λ_{uv} ~ 0.11–0.25 μm). This gives rise to larger temperature gradients in the near-surface layer and creates conditions favorable for thermomechanical destruction of the surface. This also explains the decrease in the surface damage thresholds of materials having admixture absorption bands near the bandgap absorption boundary (Fig. 2).

An important result of this experiment is justification of the need in careful removal from furnace charge and melt of molecular oxygen, lead, hydroxyl compounds and other elements, decreasing the material transparency near the bandgap absorption boundary.

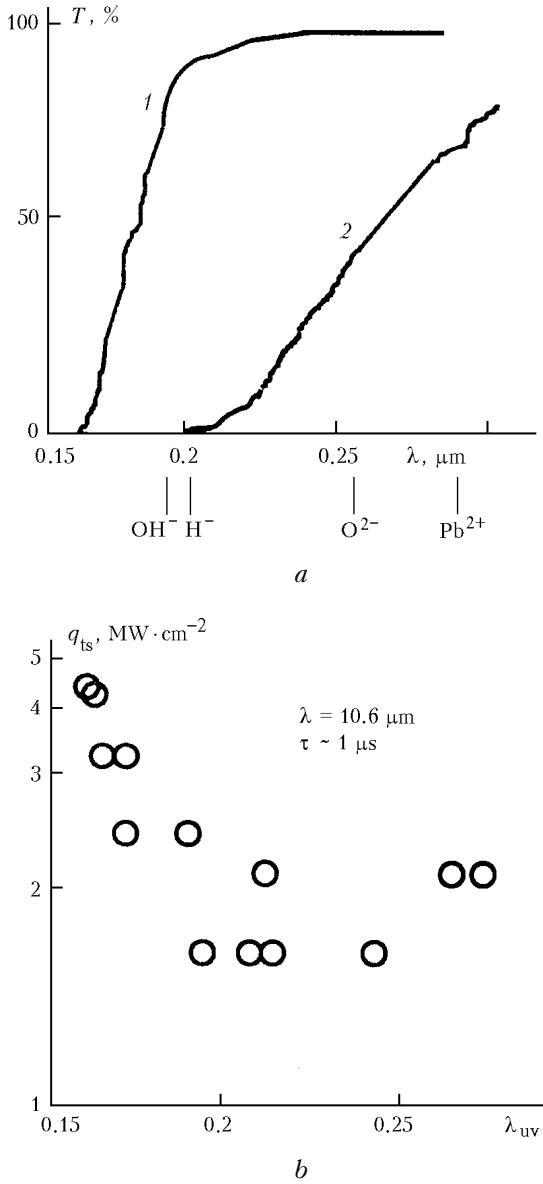

Fig. 2. Typical transmission spectra of NaCl single crystals (*a*) with very high purity (*1*) and some admixtures (*2*); dependence of the surface damage threshold on the bandgap absorption boundary (*b*).

4. In the case of laser exposure of optical elements having antireflection and protective coatings, all the above regularities keep true: the higher the reflection coefficient of the coating or substrate, the lower the surface damage threshold; if the substrate is more transparent in the near UV region (has the lower value of λ_{uv}) than the coating, then only the coating is damaged (Fig. 3).

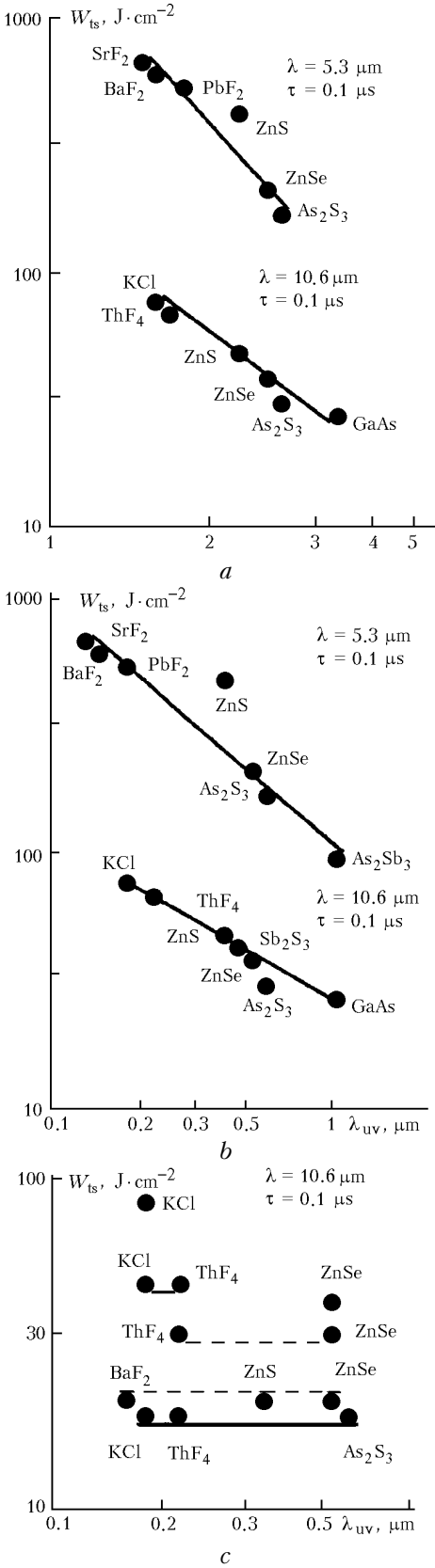

Fig. 3. Dependence of the surface damage threshold of optical elements with single-layer (*a*, *b*) and two-layer (*c*) coating on the index of refraction (*a*) and the bandgap absorption boundary (*b*, *c*) of the coating material.

Volume damage of optical elements, statistical regularities

Volume damages arising in ionic crystals under the exposure to pulsed laser radiation are local concentrators of internal stresses and look like spherical cavities of 5 to 60 μm diameter. In semiconductor crystals these cavities may be up to 100 μm in size and have a regular shape determined by the crystal symmetry; besides, the caverns of arbitrary shape, whose size may achieve ~ 0.01–3 mm, arise. The absence of caverns in ionic crystals is explained by their higher optical quality: large foreign inclusions, structure imperfections caused by deviations from the stoichiometric composition, and other growth defects are much more rare in industrial crystals. The volume damage thresholds also depend on the parameters of laser radiation and the material of an optical element, but they have somewhat higher values, than the surface damage thresholds. Under the exposure to radiation with $\lambda = 10.6$ μm and $\tau \sim 1$ μs, volume damages arose in KRS-5 single crystals at $W_{tv} \sim 1$–6, KCl – 3–10, NaCl – 4–12, BaF_2 – 10–22, CdTe – 0.5–5, ZnSe – 2–6, Ge – 3–10 J · cm^{-2} [Refs. 1, 6–9].

It was found[1,10] that the random value – the threshold of optical breakdown in the volume W_{tv} – obeys the normal distribution law and, consequently, the process of volume damage of optical materials by laser radiation is described by the Poison statistics:

$$P_v = 1 - a \exp(- bvW^2), \qquad (4)$$

where P_v is the volume damage probability; a and b are constants; v is the irradiated volume.

Therefore, the equation for dimensional dependence of the volume damage threshold W_{tv} (the so-called "dimensional effect") can be written in the general as follows

$$W_{tv} = v^{-1/2}(b^{-1} \ln a) \qquad (5)$$

or

$$W_{tv} \sim v^{-1/2}; \qquad (6)$$

$$q_{tv} \sim v^{-1/2}. \qquad (7)$$

Comparison of the experimental values and the calculated dependence $q_{tv} \sim f(v)$ for KCl and NaCl single crystals taken as an example indicates their good correlation with $v \sim 3.4 \cdot 10^{-9}$ cm^3 – $5 \cdot 10^3$ cm^3 (at the aperture ~ 80 μm–30 cm) (Refs. 4 and 7).

It was proved experimentally that the volume damage thresholds of real materials correlate with the low-frequency transmission boundary λ_{ir}, which is determined by multiphonon processes caused by simultaneous excitation of several lattice vibrational modes. For $\tau \sim 1$ μs and $v = 36$ cm^3, the observed dependence has the following form:

$$\log W_{tv} = 3.3 - 2 \log \lambda_{ir}. \qquad (8)$$

Based on these data, we have found the relation of the threshold intensity of laser radiation q_{tv} (threshold strength of the field of the light wave ε_{tv})

to the boundary frequency of the phonon spectrum $\nu_{ir} \sim \lambda_{ir}^{-1}$:

$$q_{tv} \sim \nu_{ir}^2 \quad (9)$$

or

$$\varepsilon_{tv} \sim \nu_{ir}. \quad (10)$$

Such a dependence is characteristic of the breakdown in a constant electric field (E = const), in which the mechanism of collisional avalanche ionization is realized (Fig. 4).

According to solution of the quantum kinetic equation in the diffusion approximation for the model of avalanche ionization and the case of high temperatures, the dependence of the threshold field of optical breakdown on the frequency of laser radiation ν and the speed of sound in the crystal v_s is the following:

$$\varepsilon_{tv}^2 \sim I\, v_s^2(\nu^2 + I\, l_{ac}^2), \quad (11)$$

where I is the ionization potential; l_{ac} is the electron mean free path at scattering on acoustic phonons.

The existence of the following dependences was found experimentally (Fig. 5):

at irradiation of crystals of different types by radiation at the same wavelength (ν = const)

$$\varepsilon_{tv} \sim v_s; \quad (12)$$

at irradiation of crystals of the same type (v_s = = const) by radiation at different wavelengths

$$\varepsilon_{tv} \sim \lambda^{-1}. \quad (13)$$

The results obtained can be explained most adequately within the framework of the following physical model of volume damage by laser radiation occurring in several stages[10,12]:

– optical breakdown initiation and generation of seed electrons due to ionization of an absorbing inhomogeneity;

– breakdown evolution by the type of shock avalanche ionization;

– formation of plasma on the front surface of an absorbing inhomogeneity, intense absorption of laser radiation, ionization of adjacent zones by UV radiation from the breakdown plasma;

– thermal explosion and formation of a cavity through dislocation removal of material;

– generation of the shock wave from the breakdown zone and growth of the cavity at absorption of incoming and self-focusing radiation;

– cooling of the plasma formation and stress relaxation.

The principal difference of this model is that ionization of an absorbing inhomogeneity itself is considered as a decisive factor triggering the mechanism of initiation of optical breakdown. The laser exposure of the frontal zone of the absorbing inhomogeneity causes generation of free electrons, which serve as seeds for formation and development of an electron avalanche. Energy costs for electron generation and development of the shock avalanche in the material of the absorbing inhomogeneity are obviously much lower than in the surrounding material being a wide-bandgap semiconductor or dielectric.

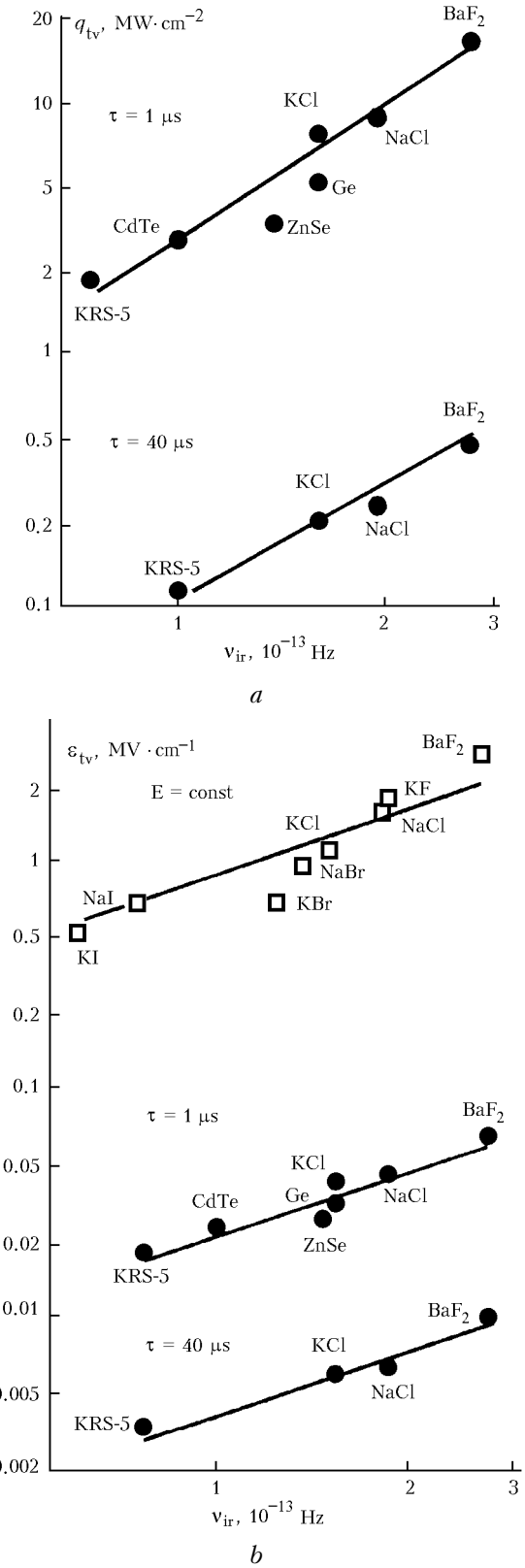

Fig. 4. Dependence of volume damage threshold (*a*) and the corresponding values of the threshold breakdown field (*b*) of semiconductor and ionic single crystals on the boundary frequency of the phonon spectrum.

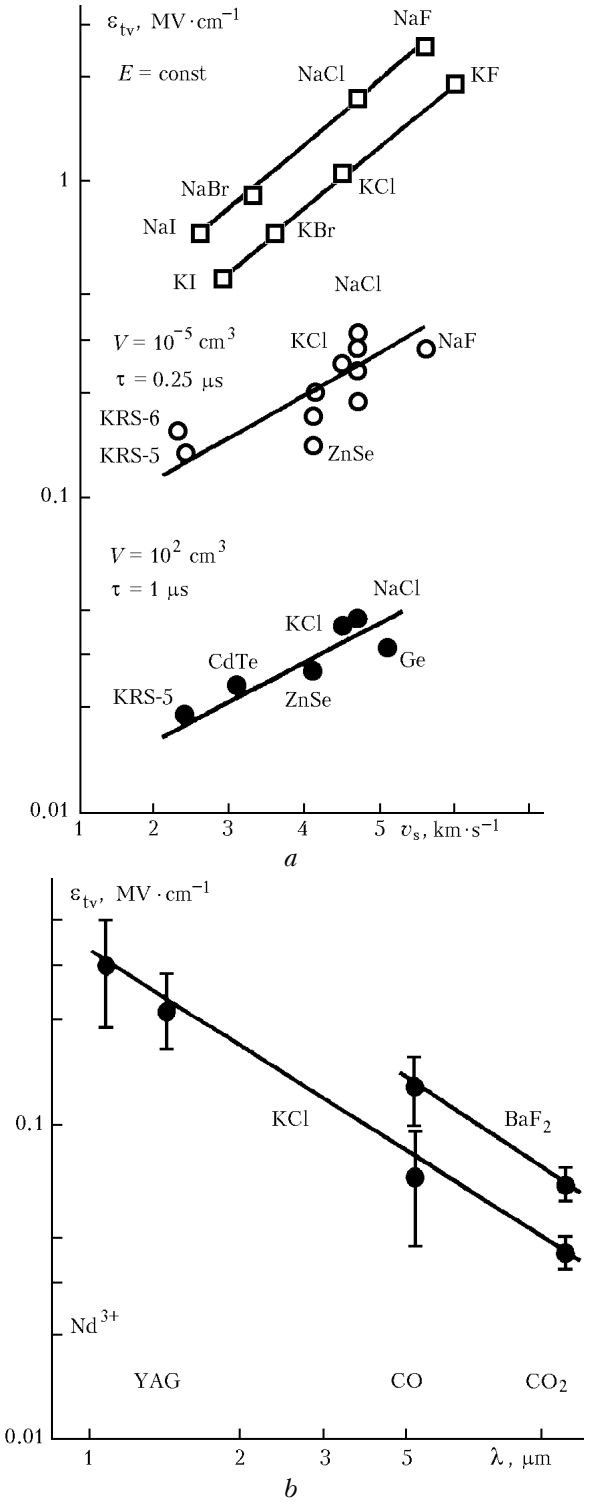

Fig. 5. Dependence of the threshold field of optical and electric breakdown on the speed of propagation of sound vibrations in the crystal (*a*) and laser radiation wavelength (*b*).

Therefore, the experimentally observed thresholds of optical breakdown of real IR materials are much lower than the breakdown thresholds calculated within the model of avalanche ionization of dielectrics in the field of the light wave and observed at focusing of laser radiation into supersmall spots. Shock avalanche ionization of the absorbing inhomogeneity leads to local plasma formation and to even more intense absorption of laser radiation and ionization of adjacent zones of the optical element material by the UV radiation emitted by the breakdown plasma.

At the following stages of the development of optical breakdown in the case that the energy absorbed by the inhomogeneity exceeds some threshold value, thermal explosion of the absorbing inhomogeneity and the surrounding material occurs with formation of a cavity. The energy costs for formation of a cavity are obviously determined by the strength of chemical bonds in the material. This is confirmed experimentally by the correlation between the threshold field of optical breakdown and the lattice energy E_p (Fig. 6), which is determined by the ionic radii of chemical elements (dependence of ε_{tv} on the total radius of anions and cations $R_A + R_C$ or the total number of the chemical elements of the material in the Periodic Table $Z_A + Z_C$).

Under continuous and quasicontinuous irradiation, the mechanisms of crystals volume damage alternate: as a result of gradual accumulation of internal stresses, KRS-5, KCl, NaCl, and Ge single crystals cleave along the cleavage planes, while BaF_2, CdTe, and ZnSe cleave along the block boundaries. The thresholds of damage under the exposure to cw CO_2 laser radiation for single crystals were the following: 1.8–3 for KCl, 0.9–2.4 for NaCl, 0.5–1.2 for KRS-5, 0.03–0.05 for BaF_2, 2–4 for ZnSe, and 1.5–2.7 kW · cm^{-2} for CdTe. These values correlate with the absorption at the working wavelength. Similar damages are observed at the exposure of ionic single crystals to repetitively pulsed radiation with the below-threshold intensity: for KCl with the total number of pulses $N \sim 10^4$–10^5 and $W \sim 0.5$–4 J·cm^{-2}, and for BaF_2 — $N \sim 10^3$–10^4 and $W \sim 1$–6 J · cm^{-2} (Refs. 1 and 3).

The difference between the damage mechanisms of optical materials in the case of cw and pulsed laser radiation causes different approaches to improvement of their laser-radiation tolerance.

It was found that under the exposure to laser radiation with $\tau \le 0.5$–1 ms and $\lambda = 10.6$ μm, as well as $\tau \le 5$–10 μs and $\lambda = 1.06$ μm the crystal damage is caused by optical breakdown at absorbing inhomogeneities accompanied by the fast process of re-distribution of the internal stresses that manifests itself in periodic alternation of the birefringence pattern. The exposure to radiation with $\tau \ge 0.1$ s causes thermomechanical damage of the material, and at irradiation by laser pulses with $\tau \sim 1.5$–5 ms and $\lambda = 1.06$ μm the peculiarities of the damage are determined by the intensity of incoming laser radiation — internal stresses are accumulated gradually at the below-threshold intensity. Alternation of the mechanism of destruction by laser radiation at variation of the pulse duration occurs at the pulse duration ~ 1–10 ms (Fig. 7) (Refs. 1 and 5).

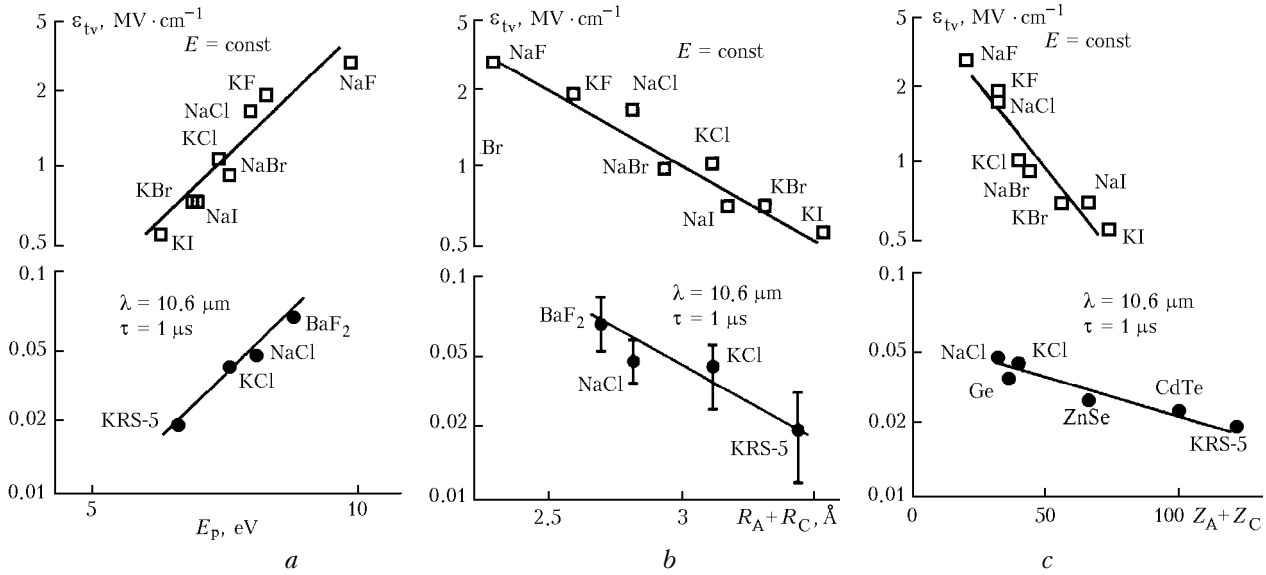

Fig. 6. Dependence of the threshold field of optical and electric volume breakdown on the bond energy (*a*), total radius (*b*), and the total number (*c*) of material anions and cations in the Periodic Table.

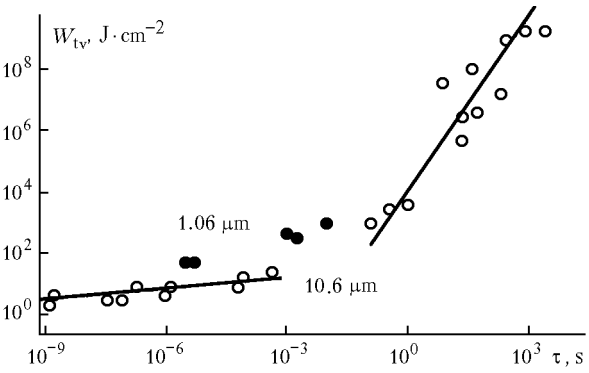

Fig. 7. Dependence of the volume damage threshold of KCl single crystals on duration of laser pulse with the wavelength of 10.6 (○) and 1.06 μm (●).

Based on the results of investigations carried out, we have formulated the main principles, to be followed in developing wide-aperture optics of high-power mid-IR lasers, selecting the material of an optical element, technology of its fabrication, methods to improve the laser-radiation tolerance of materials, and to optimize the design of optical elements.[10–12]

• The material of an optical element should have as low as possible reflectivity and index of refraction, as well possibly lower absorption bandgap boundary, the largest bandgap, and high mechanical characteristics. The low-frequency boundary of the transmission spectrum should lie near the laser radiation wavelength. In a series of chemical compounds of the same class, the laser-radiation tolerance increases with the decrease of the anion and cation radii of elements or the decrease of their total number in the Periodic Table.

• The technology of production of IR materials should provide for the highest optical quality and the lowest concentration of admixtures having absorption bands near the material absorption bandgap boundary.

• The conditions of irradiation determine application of technological and design methods for improving the laser-radiation tolerance of the material: in the case of cw irradiation the laser-radiation tolerance and service life can be increased due to chemical, laser, and thermal processing of the material, as well as application of technologies improving its mechanical characteristics, while at pulsed irradiation these parameters can be increased due to the use of methods decreasing the irradiated volume, improving the uniformity of intensity distribution in the cross section of wide-aperture laser radiation, as well as due to combined application of technological and design methods.

References

1. S.G. Kazantsev, Izv. Vyssh. Uchebn. Zaved., Ser. Fiz., No. 10, 68–84 (1998).
2. S.G. Kazantsev, Kvant. Elektron. **25**, No. 4, 333–336 (1998).
3. S.G. Kazantsev, Kvant. Elektron. **25**, No. 6, 555–557 (1998).
4. S.G. Kazantsev, Kvant. Elektron. **24**, No. 3, 269–270 (1997).
5. S.G. Kazantsev, Kvant. Elektron. **24**, No. 3, 271–273 (1997).
6. S.G. Kazantsev, A.A. Blistanov, O.M. Kugaenko, and B.C. Petrakov, Kristallografiya **44**, No. 4, 689–693 (1999).
7. A.A. Blistanov, S.G. Kazantsev, and O.M. Kugaenko, Izv. Vyssh. Uchebn. Zaved., Ser. Mater. Elektron. Tekhn., No. 1, 4–15 (2002).
8. S.G. Kazantsev, Opt. Zh. **64**, No. 6, 63–65 (1997).
9. S.G. Kazantsev, Kristallografiya **44**, No. 5, 894–896 (1999).
10. S.G. Kazantsev, in: *Tech. Digest "Russian-German Laser Symposium-2000,"* (Vladimir–Suzdal, 2000), p. 45.
11. S.G. Kazantsev, in: *Proc. of VII Int. Conf. on Laser and Laser-Information Technologies: Basic Applications,"* (Vladimir–Suzdal–Shatura, 2001), p. 78.
12. S.G. Kazantsev, in: *Abstracts of Reports at V Intern. Conf. AMPL'2001* (Tomsk, 2001), pp. 107–108.